Chinese Journal of Natural Medicines

The extract of *Cyperus rotundus* rhizome promotes hair growth and modulates hair cycle *in vivo* and *in vitro*

Yunwei Hu, Keke Hu, Jiaying Liang, Xingjiang Zhang, Huijuan Li, Jianxin Wu, Qing Huang

Citation: Yunwei Hu, Keke Hu, Jiaying Liang, Xingjiang Zhang, Huijuan Li, Jianxin Wu, Qing Huang, The extract of *Cyperus rotundus* rhizome promotes hair growth and modulates hair cycle *in vivo* and *in vitro*, Chinese Journal of Natural Medicines, 2026, 24(2), 203−214. doi: 10.1016/S1875−5364(26)61091−6.

View online: https://doi.org/10.1016/S1875−5364(26)61091−6

Chinese Journal of Natural Medicines 24 (2026) 203-214

Contents lists available at ScienceDirect

Chinese Journal of Natural Medicines

journal homepage: www.cjnmcpu.com/

Original article

The extract of *Cyperus rotundus* rhizome promotes hair growth and modulates hair cycle *in vivo* and *in vitro*

Yunwei Hu, Keke Hu, Jiaying Liang, Xingjiang Zhang, Huijuan Li, Jianxin Wu*, Qing Huang*

Skin Health and Cosmetic Development & Evaluation Laboratory, China Pharmaceutical University, Nanjing 211198, China

ARTICLE INFO

Article history:
Received 25 January 2025
Revised 18 April 2025
Accepted 6 July 2025
Available online 20 February 2026

Keywords:
Cyperus rotundus
Hair growth
Hair cycle
Wnt/*β*-Catenin

ABSTRACT

Hair loss, a multifactorial disorder characterized by follicular miniaturization and excessive shedding, significantly impairs psychological well-being and quality of life. *Cyperus rotundus* rhizome (CR), a traditional Chinese medicine used for various ailments, has not been evaluated for efficacy in treating hair loss. This study presents the first comprehensive assessment of the hair growth-promoting effects of ethanol extract from CR on mouse primary dermal papilla cells (MDPCs) and human immortalized hair DPCs (IHHDPCs), employing cell counting kit-8 (CCK-8), scratch assay, reverse transcription-quantitative polymerase chain reaction (RT-qPCR), and Western blot (WB). CR treatment activated the Wnt/*β*-Catenin signaling pathway by upregulating Wnt10b, increasing *β*-Catenin protein levels and promoting its nuclear translocation, while simultaneously downregulating transforming growth factor-beta 1 (TGF-β1), BMP4, and dickkopf-related protein 1 (DKK1) in MDPCs. These molecular changes enhanced cell proliferation and increased secretion of key growth factors—insulin-like growth factor 1 (IGF1), keratinocyte growth factor (KGF), and vascular endothelial growth factor (VEGF)—thereby stimulating hair growth and prolonging the anagen phase, which was confirmed in an *ex vivo* hair follicle (HF) organ culture model. Chromatographic analysis identified the petroleum ether fraction (CRP), enriched in sesquiterpenes, as the primary bioactive component. Both CR and CRP promoted IHHDPC proliferation, migration, and growth factor expression through activation of the Wnt/*β*-Catenin pathway, with CRP exhibiting superior bioactivity. Furthermore, both treatments stimulated HF cycling, increased follicular density, and upregulated Ki67 and *β*-Catenin expression in the dorsal skin of C57BL/6 mice. Collectively, these findings demonstrate that CR and CRP promote hair growth and modulate the hair cycle *via* enhancement of Wnt/*β*-Catenin signaling, providing a scientific basis for the potential clinical application of *C. rotundus* rhizomes in hair loss therapy and the development of related pharmaceuticals or cosmetics.

1. Introduction

Although hair loss does not directly affect physical health, it significantly impairs mental well-being and has attracted widespread attention [1]. Hair growth proceeds in cycles, transitioning through the anagen, catagen, and telogen phases [2]. The anagen phase is characterized by hair follicle (HF) cell proliferation, expansion of the follicle, downward migration of the niche into the dermal white adipose tissue (dWAT), and continuous elongation of the hair shaft (HS) [3, 4]. The catagen phase represents a transitional stage during which cell proliferation and differentiation cease, and HS elongation halts. During the telogen phase, the HS forms a club-shaped structure and is eventually shed, while changes in regulatory factor expression prepare the follicle for the next growth cycle [5].

In the HF cycle, activation occurs sequentially *via* signaling pathways such as Wnt/*β*-Catenin and BMP, which regulate downstream signals and drive the intrinsic "autonomous clock" of the hair cycle through autocrine and paracrine mechanisms in cells [6]. The dermal papilla (DP) is a multicellular structure located within the hair bulb that supplies essential nutrients for HF growth *via* its capillaries and dermal papilla cells (DPCs) [7]. DPCs are specialized mesenchymal fibroblasts that play a pivotal role in regulating hair growth and cycling [8]. These cells secrete growth factors—including insulin-like growth factor 1 (IGF1), keratinocyte growth factor (KGF), vascular endothelial growth factor (VEGF)—that promote capillary formation within the DP, stimulate epithelial cell proliferation and differentiation, and enhance epithelial-mesenchymal interactions critical for HF development [9].

The Wnt/*β*-Catenin pathway is activated early in the anagen phase, facilitating HF regeneration, development, and maintenance of anagen [10, 11]. Among Wnt ligands, Wnt10b plays a central role in the mammalian HF cycle, showing high expression during anagen and suppression during telogen; overexpression of Wnt10b can shift HFs from a refractory to an inducible state, triggering the onset of anagen [12, 13]. *β*-Catenin, a key transducer in the

* Corresponding author.
E-mail addresses: wujianxin@cpu.edu.cn (J. Wu); huangqing@cpu.edu.cn (Q. Huang)

https://doi.org/10.1016/S1875-5364(26)61091-6

Wnt pathway, is highly expressed in DPCs, where it translocates to the nucleus, activates the lymphoid enhancer-binding factor/T-cell factor (LEF/TCF) complex, and regulates transcription of downstream genes [14]. This process promotes cell proliferation, migration, and secretion of growth factors such as IGF1, KGF, and VEGF [15]. Conversely, dickkopf-related protein 1 (DKK1), an endogenous inhibitor of Wnt signaling, is upregulated during catagen and telogen, thereby suppressing Wnt/*β*-Catenin signaling [16, 17]. The BMP signaling pathway is predominantly active during catagen and telogen. BMP4, a member of the transforming growth factor-beta (TGF-β) superfamily produced by DPCs, reaches peak expression in telogen and declines during early anagen [18]. Elevated BMP4 levels maintain HFs in a refractory state, preventing responsiveness to regenerative Wnt/*β*-Catenin signals [19]. Furthermore, TGF-β1, a well-established inhibitor of hair growth, induces apoptosis and promotes HF regression [20]. Additionally, BMP-mediated inhibition of Wnt signaling is associated with increased DKK1 expression [6, 18]. Although the direct link between BMP4 and DKK1 in HF cycle regulation remains unclear, BMP4's role as an upstream regulator of DKK1 in inhibiting Wnt/*β*-Catenin signaling has been extensively documented in bone formation and idiopathic pulmonary fibrosis [21, 22].

A healthy scalp typically maintains approximately 90% of HFs in the anagen phase, 1% in catagen, and 9% in telogen [5]. However, disruptions to the normal HF cycle caused by stress, medications, or hormonal imbalances can increase the proportion of follicles in telogen, reduce hair density, and ultimately lead to baldness [23]. Currently, only minoxidil and finasteride are FDA-approved treatments for hair loss; however, their limited efficacy and potential adverse effects fail to fully meet patient needs [24]. Hair loss generally progresses gradually, highlighting the importance of enhancing the growth phase and cyclical renewal of HFs at early stages to prevent further deterioration. Recently, natural compounds have gained increasing recognition for their safety and multifaceted therapeutic potential in HF regeneration, prompting significant interest in identifying bioactive constituents from plant extracts capable of promoting hair growth for anti-hair loss product development [1, 25]. Fish collagen peptides enhance DPC proliferation and growth factor expression by upregulating Wnt/*β*-Catenin signaling while downregulating BMP4, DKK1, and the inhibitory factor TGF-β, a modulation shown to promote dorsal hair growth in C57BL/6 mice [26]. Similarly, anemarrhena saponin BII (0.5%) increases hair regeneration area and HF density in mouse models, with mechanistic studies indicating its ability to upregulate *β*-Catenin and Wnt10b expression in dorsal skin [27]. Additionally, ginseng extract and its active components (ginsenosides Rb1, Rg1, and Re) have been demonstrated to promote HS elongation in *ex vivo* HF organ culture systems, inhibit BMP4 expression in DPCs, and stimulate the transition from telogen to anagen [28].

Traditional Chinese medicine has been used for thousands of years to treat hair loss, accumulating extensive clinical experience. *Cyperus rotundus* rhizomes (CR), known as Xiangfu in traditional Chinese medicine, possess diverse biological activities, making them valuable for healthcare applications [29]. Recent studies have elucidated the pharmacological effects, phytochemistry, biological activities, safety, and applications of CR, revealing anti-inflammatory, anti-oxidant, anti-depressant, anti-diabetic, neuroprotective properties, as well as their capacity to regulate irregular menstruation [30]. Although the ancient Chinese medical text Hongjing Tao's *Ming Yi Bie Lu* documented the beneficial effects of CR on hair growth and included them in prescriptions for treating hair loss [17], no scientific studies have evaluated their hair growth-promoting activity or identified the underlying bioactive components. In this study, we investigated, for the first time, the activity of CR in regulating and promoting hair growth during the HF cycle using both *in vitro* and *in vivo* models. We demonstrate that the hair growth-promoting effects of CR involve mediation and modulation of the Wnt/*β*-Catenin pathway, with sesquiterpenoids likely playing a major role.

2. Materials and methods

2.1. Materials

Minoxidil and DHT were purchased from Beijing Solarbio Technology Co., Ltd. (Beijing, China). Cyperenone and *α*-cyperone were obtained from Chengdu Pufei De Biotechnology (Chengdu, China). Nootkatone was bought from Chengdu Must Biotechnology (Chengdu, China). MSAB was bought from MedChemExpress (Shanghai, China). Human DKK1 protein was purchased from SinoBiological (Beijing, China). Mouse Wnt10B antibody (MAB2110) was purchased from R&D Systems (Minneapolis, MN, USA). *α*-Smooth muscle actin (*α*-SMA) (14395-1-AP), *β*-Catenin (51067-2-AP), and DKK1 (21112-1-AP) antibodies were obtained from Proteintech (Wuhan, China). *α*-Tubulin rabbit mAb (AC049), TGF beta rabbit pAb (A2124), and BMP4 rabbit pAb (A1565) were bought from ABclonal (Wuhan, China). Alexa Fluor 488 AffiniPure goat anti-rabbit IgG (H + L) and goat anti-rabbit IgG HRP were obtained from Biosharp (Anhui, China). The BCIP/NBT alkaline phosphatase (ALP) staining kit was purchased from Beyotime (Shanghai, China). Mouse VEGFA enzyme-linked immunosorbent assay (ELISA) kit was purchased from ABclonal (Wuhan, China). All reagents or kits were used according to the manufacturer's instructions.

2.2. Extraction and isolation of CR

CR was purchased from Bozhou Chinese Medicinal Market, and identified by Prof. Qing Huang from the School of Traditional Chinese Medicine of China Pharmaceutical University. The rhizomes were chopped using a high-speed cutter, soaked in 75% ethanol for 24 h, and ultrasonically extracted three times at 50 °C for 1 h each. The extract was filtered under reduced pressure and concentrated to dryness using a vacuum rotary evaporator to obtain CR, yielding 13% of the original rhizome mass.

Following a polarity gradient, petroleum ether, ethyl acetate, and *n*-butanol were sequentially used to partition the CR water suspension, yielding the petroleum ether extract (CRP), ethyl acetate extract (CRE), *n*-butanol extract (CRB), and water raffinate (CRW), with yields of 24%, 12%, 8%, and 56% of the CR mass, respectively. CRP was further separated by silica gel column chromatography and eluted with CH_2Cl_2–MeOH mixtures (50∶1 to 1∶1) to afford fractions CRP-1, CRP-2, CRP-3, CRP-4, and CRP-5, with yields of 2.9%, 1.4%, 20.5%, 20.5%, and 44.8% of the CRP mass, respectively.

2.3. LC analysis

2.3.1. Chromatographic conditions

CR extracts and fractions were analyzed using Diamonsil Plus C_{18} (4.6 mm × 250 mm, 5 μm) or Hedera ODS-2 (4.6 mm × 250 mm, 5 μm) columns. The mobile phase consisted of water (A) and methanol (B). The elution program was as follows: 0–10 min, 40%–48% B; 10–45 min, 48%–58% B; 45–65 min, 58%–62% B; 65–75 min, 62%–65% B; 75–90 min, 65%–80% B. The flow rate was maintained at 1 mL·min^{-1}, with a column temperature of 40 °C. Samples were injected at a concentration of 2 mg·mL^{-1} and an injection volume of 10 μL.

2.3.2. Mass spectrometry conditions for electrospray ionization (ESI)-quadrupole-time-of-flight (Q-TOF) tandem mass spectrometry (MS/MS) analysis of CR

ESI-Q-TOF MS/MS analysis was conducted on an Agilent

1290 Infinity liquid chromatography (LC) system coupled to an Agilent 6545 Q-TOF mass spectrometer. ESI was performed in both negative and positive ionization modes, and data for positive and negative ions with m/z values ranging from 100 to 1700 were collected. Fixed collision energies of 10, 30, 50, and 70 eV were applied for MS/MS analysis. Data were processed using Agilent MassHunter Qualitative Analysis software.

2.4. Isolation and identification of primary mice dermal papilla cells (MDPCs)

We optimized the enzymatic digestion method for isolating DPs to simplify the procedure and improve reproducibility [31-34]. The protocol is outlined in Fig. S1 (Supporting information). The isolated cells were identified based on morphology and expression of α-SMA and ALP markers (Fig. S2) [31, 35]. MDPCs from the 2nd to 4th passages were used in experiments.

2.5. Cell culture and cell viability

MDPCs, immortalized human hair DPCs (IHHDPCs, ABM, Canada), human immortal keratinocyte line (HaCaT, Meisen, Zhejiang, China), and human umbilical vein endothelial cells (HUVEC, Shanghai Institute of Cell Biology, China) were cultured in DMEM medium (Mersen, Zhejiang, China), with 10% FBS (Gibco, US) and 1% penicillin-streptomycin (NCM Biotech, Suzhou, China), at 37 °C in a 5% CO_2 incubator. Cell viability was assessed using the CCK8 assay according to the manufacturer's instructions (Vazyme, Nanjing, China), and measured using a Spectra Max 190 microplate reader (Molecular Devices) at a wavelength of 450 nm. A preliminary dose-response experiment on MDPC revealed that CR concentrations of 100 μg·mL^{-1} and above exhibited strong cytotoxicity, while 50 μg·mL^{-1} was identified as the safe concentration limit.

2.6. EdU staining

After 24 h of treatment, cell proliferation was assessed using the BeyoClick™ EdU cell proliferation kit with Alexa Fluor 555 according to the manufacturer's instructions and visualized under a fluorescence microscope (Guangzhou Micro-shot Technology Co., Ltd., MSHOT MF53-N).

2.7. Ribonucleic acid (RNA) extraction and reverse transcription-quantitative polymerase chain reaction (RT-qPCR)

Cells were harvested after 24 h of treatment and lysed with TRIzol to extract total RNA following the reagent protocol (Accurate Biology, China). cDNA synthesis and RT-qPCR were performed per the manufacturer's instructions (Vazyme, Nanjing, China). Primer sequences are listed in Table S1.

2.8. Western blot (WB)

After 24 h of treatment, cells were lysed using RIPA buffer (R0010, Solabo, Beijing) and subjected to high-speed centrifugation to collect protein samples. Proteins were separated by electrophoresis, transferred to membranes, and detected using ECL reagent on an imaging system (Tanon, China). Detailed procedures followed previously published protocols [36].

2.9. Immunofluorescence assay

MDPCs were seeded in six-well plates. After adherence, serum-free medium was used to starve cells for 12 h. Cells were treated with CR or minoxidil for 1 h. Intracellular β-Catenin was labeled with β-Catenin antibody and fluorescent secondary antibody, and nuclei were stained with DAPI. Fluorescence microscopy was used for detection.

2.10. Mice vibrissa HFs organ ex vivo culture

Vibrissa HFs from 5-week-old C57BL/6 mice were isolated, retaining only intact follicles in anagen phase IV/V [37]. HSs above the epidermis were trimmed, and two follicles were placed per well in a 24-well plate. They were randomly assigned to six groups (n = 20–24): control (vehicle), 6.25 μg·mL^{-1} CR, 12.5 μg·mL^{-1} CR, 100 μmol·L^{-1} minoxidil, 10 μmol·L^{-1} DHT, and 12.5 μg·mL^{-1} CR + 10 μmol·L^{-1} DHT. All samples were dissolved in William's E medium (Procell, Wuhan, China) containing 2 mmol·L^{-1} L-glutamine (Solarbio, Beijing), 10 μg·mL^{-1} insulin (Solarbio, Beijing), 5 ng·mL^{-1} hydrocortisone (OriLeaf, Shanghai), and 1% penicillin-streptomycin; 400 μL of solution was added to each well [37]. Images were captured under a stereomicroscope at consistent magnification on days 0, 1, 2, 3, and 4 for subsequent data analysis.

2.11. Scratch assay

IHHDPCs were seeded into six-well plates pre-marked with horizontal lines. Upon reaching 100% confluence, a scratch was made across the monolayer. After removing floating cells with PBS washes, culture medium with or without 25 μg·mL^{-1} CR, CRP, or 10 μmol·L^{-1} minoxidil was added. Scratch widths at the intersection points were recorded and compared under an optical microscope at 0 and 30 h post-treatment.

2.12. Hair loss mice model establishment and trial grouping

Male C57BL/6 mice (6–7 weeks old) were purchased from Jiangsu Qinglongshan Biotechnology Co., Ltd. (Jiangsu, China) and housed under a 12-h light-dark cycle. All animal procedures were approved by the Institutional Animal Ethics Committee of China Pharmaceutical University (approval number: 2024-02-013). Given the differences between *in vitro* and *in vivo* settings, dosage ranges were referenced from literature on topical application of plant extracts in mice [38]. The pilot experiment preceded the formal study to confirm efficacy and absence of adverse effects on body weight. Following one week of acclimatization, mice were randomly divided into six groups: Control (solvent); Minoxidil (2.5% minoxidil in solvent); CRL (1.25% CR in solvent); CRH (2.5% CR in solvent); CRPL (1.25% CRP in solvent); CRPH (2.5% CRP in solvent). Hair was removed using 3 cm × 5 cm wax strips to expose uniform dorsal skin areas under anesthesia. Test solutions were prepared in a mixture of 60% ethanol, 38% propylene glycol, and 2% DMSO, and 200 μL was applied topically daily for 21 d (n = 12). Photographs were taken under avertin anesthesia (Nanjing Aibi Biotechnology Co., Ltd., Nanjing, China) on days 0, 7, 14, and 21 post-depilation. Skin samples were collected on days 0, 7, 10, 14, and 21 post-depilation for histological analysis.

2.13. Histological analysis and immunohistochemistry analysis

Mouse skin samples were fixed in 4% paraformaldehyde, embedded in paraffin, and sectioned. Paraffin sections were stained with hematoxylin and eosin (H&E) and Masson's trichrome. Immunohistochemical analysis was performed to detect Ki67 and β-Catenin using specific antibodies.

2.14. Statistical analysis

Data were analyzed using GraphPad Prism 9.5 and are presented as mean ± standard deviation (SD). One-way analysis of variance (ANOVA) and two-tailed Student's t-test were used to determine statistical differences between groups. A P value < 0.05

was considered statistically significant.

3. Results and discussion

3.1. Chemical characterization of CR

Cyperus rotundus contains various bioactive compounds, including flavonoids, phenolic acids, and terpenoids, which have garnered considerable attention due to their biological activities. A review by Xue et al. summarized 522 components identified in *Cyperus rotundus* in recent years [30]. In this study, 61 sesquiterpenoids (including 3 sesquiterpenoid alkaloids), 7 flavonoids, 4 phenolic acids, and 1 *β*-hydroxy acid with its derivatives were tentatively identified. Identification was based on analysis of retention times and *m/z* values of precursor and fragment ions from LC-MS/MS data, supported by literature references and natural product databases, with a mass accuracy error threshold. Representative sesquiterpenoids—cyperenone, *α*-cyperone, and nootkatone—were confirmed using authentic standard samples. The total ion chromatogram (TIC) is shown in Fig. S3, and the identified constituents along with corresponding fragment ions are listed in Tables S2 and S3. Additionally, an high performance liquid chromatography (HPLC) method was established to quantify the major components—cyperenone, *α*-cyperone, and nootkatone—to ensure consistency in administration. The assay methodology and results for these compounds are provided in Fig. S4 and Table S4.

3.2. Effects of CR on cell viability

DPCs play a pivotal role in HF morphogenesis and regeneration [25]. The proliferative capacity of DPCs determines the size of the DP, which is a key factor influencing HF size, type, and HS diameter [39]. Epithelial cells proliferate and differentiate to participate in HF formation, while capillaries expand to support HF nutrition [40, 41]. To evaluate the effect of CR on cell viability, a CCK-8 assay was performed. EdU staining was also conducted to quantify the proliferation rate of MDPCs. The results (Figs. 1A–1C) showed that, compared with the control group, MDPC viability significantly increased after treatment with 6.25–50 μg·mL^{-1} CR for 24 h, with the most pronounced increase (132.7%) observed at 12.5 μg·mL^{-1} CR. EdU staining further confirmed a significant, dose-dependent increase in the number of EdU(+) cells following CR treatment. Moreover, CR treatment significantly enhanced the viability of HaCaT and HUVEC cells (Figs. 1D and 1E), which may support HF development and nutrient supply.

3.3. CR upregulated the expression of growth factors

DPCs regulate the HF cycle transition through autocrine and paracrine signaling. Growth factors such as IGF1, KGF, and VEGF are highly expressed during the anagen phase and promote cell proliferation, HF development, and maintenance [42, 43]. We investigated the effects of CR on the expression of *Igf1*, *Kgf*, and *Vegf* in MDPCs using RT-qPCR and quantified VEGF secretion *via* ELISA. The results (Figs. 1F–1H) showed that treatment with 12.5

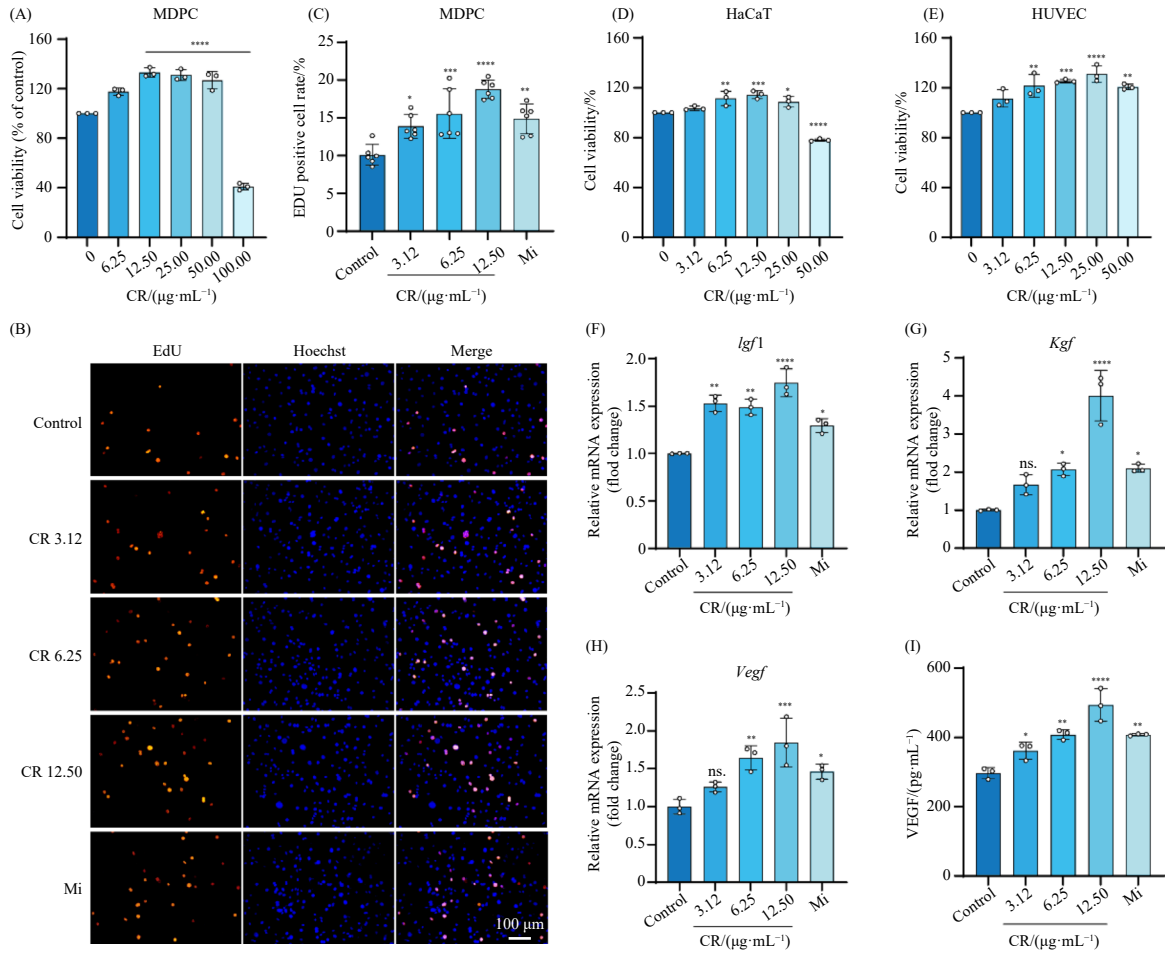

Fig. 1 Effects of CR on cell viability and growth factors secretion in MDPC. (A, D, E) The effects of CR on MDPC, HaCaT and HUVEC viability. (B) MDPC proliferation ability *via* EdU assay, EdU(+) in red and cell nucleus in blue. (C) Quantification of the EdU(+) cells rate in (B). Relative mRNA expression of *Igf1* (F), *Kgf* (G), and *Vegf* (H) in MDPC. (I) Quantified the secretion of VEGF by Elisa assay. The data were expressed as mean ± SD (n = 3–5). $^{*}P < 0.05$, $^{**}P < 0.01$, $^{***}P < 0.001$, $^{****}P < 0.0001$ *vs* control by ANOVA. Mi: minoxidil, as a positive control.

μg·mL^{-1} CR upregulated the relative messenger RNA (mRNA) expression of *Igf1*, *Kgf*, and *Vegf* by 1.74-fold, 4.01-fold and 1.99-fold respectively. Additionally, extracellular VEGF secretion increased significantly in a dose-dependent manner compared to the control group (Fig. 1I).

3.4. Effect of CR on the balance of positive and negative regulators in MDPCs

Multiple molecular signaling pathways are involved in HF development and cycling. The Wnt/β-Catenin pathway promotes HF development and maintains the growth phase, whereas BMP4, TGF-β1, and DKK1 induce HF regression [2, 20, 44-46].

To examine the effects of CR on positive regulators (Wnt10b and β-Catenin) and negative regulators (BMP4, TGF-β1, and DKK1) in MDPCs, we employed RT-qPCR and WB analysis, along with immunofluorescence co-localization to assess nuclear β-Catenin levels. The results (Figs. 2A–2E) showed that, compared with the control group, CR upregulated *Wnt10b* and *β-Catenin* mRNA expression and increased protein levels of Wnt10b and β-

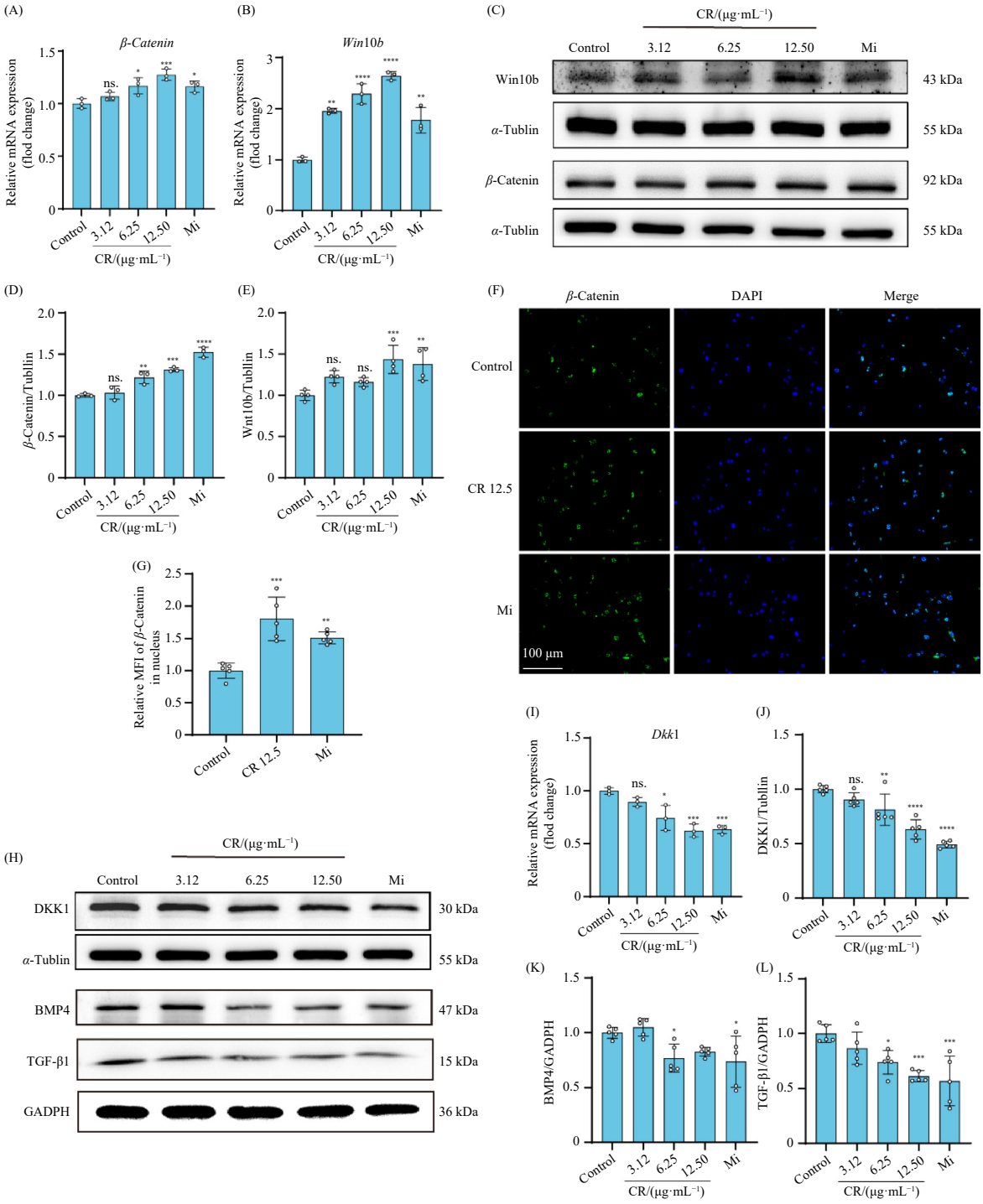

Fig. 2 Effects of CR on the Wnt/β-Catenin pathway, DKK1, BMP4 and TGF-β1 in MDPCs. (A and B) Effects of CR on the mRNA expression levels of *Wnt10b* and *β-Catenin* (n = 3). (C–E) Effects of CR on the protein levels of Wnt10b and β-Catenin and quantification of the relative gray value density (n = 3–4). (F) Immunofluorescence analysis of β-Catenin nuclear translocation following CR treatment. β-Catenin is labeled in green, and the nuclear region is labeled in blue. (G) Quantification of the relative mean fluorescence intensity of β-Catenin in the nucleus. (H, J–L) Effects of CR on the protein level of DKK1, BMP4 and TGF-β1, and its quantification (n = 5). (I) Effects of CR on the mRNA expression level of *Dkk1*. The data were expressed as mean ± SD. $^{*}P < 0.05$, $^{**}P < 0.01$, $^{***}P < 0.001$, $^{****}P < 0.0001$ *vs* control by ANOVA.

Catenin in a dose-dependent manner. Cells treated with 12.5 μg·mL^{-1} CR exhibited increased nuclear accumulation of *β*-Catenin (Figs. 2F and 2G). Furthermore, CR treatment downregulated the protein levels of DKK1, BMP4, and TGF-β1 in MDPCs, as well as the transcription level of *Dkk1* mRNA (Figs. 2H–2L). These findings indicate that CR maintains the anagen phase and alleviates HF regression by activating the Wnt/*β*-Catenin signaling pathway and suppressing the inhibitory signals mediated by TGF-β1, BMP4 and DKK1.

3.5. Effects of CR on ex vivo-cultured mice vibrissa HF organ

Previously, we explored the potential of CR to promote HF growth and modulate the HF cycle at the cellular level. Since *ex vivo*-cultured mouse vibrissa HFs maintain HS elongation and cycle transitions similar to those observed *in vivo* [37, 47], the effect of CR was further evaluated using this model. Randomly grouped mouse vibrissa HFs were photographed on days 0, 1, 2, 3, and 4 of treatment. HS elongation and the proportion of HFs in anagen and catagen phases were recorded. By day 3, visible changes in HF morphology were observed across groups Fig. 3A. HS elongation was measured (Fig. 3B): average HS length increased to 548 μm in the control group, whereas treatment with 6.25 and 12.5 μg·mL^{-1} CR, as well as minoxidil, resulted in HS elongation to 822.3, 936.0, and 794.0 μm, respectively, indicating that both CR and minoxidil accelerated HS extension. In contrast, DHT treatment significantly inhibited HS extension in *ex vivo*-cultured mouse vibrissa HFs, but this inhibition was reversed when CR was co-administered.

Ex vivo-cultured HFs undergo regression, characterized by separation of the HS from the DP. Based on the distance between the HS and DP, HFs were classified into anagen, early catagen, and late catagen phases (Fig. 3C) [37, 48]. The data showed that over 70% of HFs remained in the anagen phase after 3 days of treatment with CR or minoxidil, compared to 62% in the control group. Consistent with previous reports [37], DHT exacerbated HF regression, with only 52% of HFs in the anagen phase and 41% in the late catagen phase. However, with concurrent CR treatment, the proportion of HFs in the late catagen phase decreased to 26%. These results demonstrate that CR prolongs the anagen phase and counteracts DHT-induced HF regression.

3.6. Effects of CR extracts and fractions on IHHDPC

To identify the active constituents in CR responsible for promoting hair growth, a stepwise extraction was performed Fig. 4A,

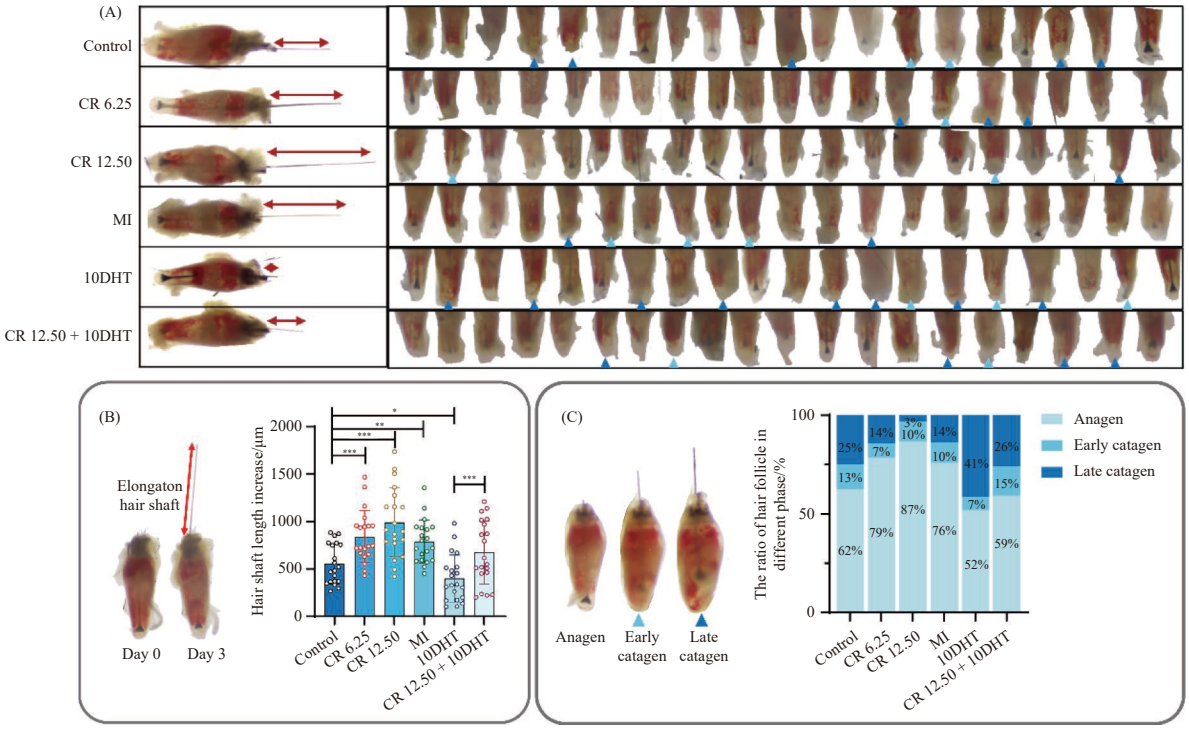

Fig. 3 Effects of CR *ex vivo*-cultured mice vibrissa HFs (n = 20). (A) Representative mice vibrissa HFs of each group after 3 d *ex vivo*-culture. (B) Effects of CR on the increase of HS length of HFs. Data are presented as mean ± SD. $^{*}P < 0.05$, $^{**}P < 0.01$, $^{***}P < 0.001$ by two-tailed Student's *t*-test. (C) Effects of CR on the cycle transition of HFs.

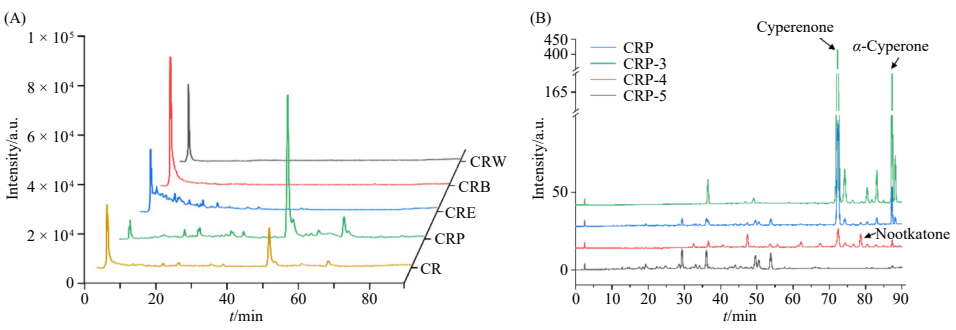

Fig. 4 HPLC analysis of CR extracts and fractions at UV_{254nm}. (A) CR extracts were separated using a Diamonsil Plus C_{18} (4.6 mm × 250 mm, 5 μm) column. (B) CRP fractions were separated using a Hedera ODS-2 (4.6 mm × 250 mm, 5 μm) column.

enabling effective separation of each extract. Based on LC-MS/MS and HPLC-UV analyses, flavonoids and phenolic acids were enriched in the CRE fraction, whereas sesquiterpenoids were enriched in CRP. The effects of CR and its four extracts on the viability of IHHDPCs were assessed using the CCK-8 assay. As shown in Fig. 5A, CR enhanced IHHDPC viability, with CRP exhibiting the highest activity among the four extracts. Treatment with 50 μg·mL^{-1} CRP increased IHHDPC viability to 175%. Although flavonoids such as quercetin and luteolin in CRE have been reported to stimulate DPC viability [49, 50]. CRE did not show significant activity in our study, likely due to low concentrations of these compounds. EdU staining and scratch assays were performed on IHHDPCs treated with CR and CRP (Figs. 5B–5E). Compared with the control group, the EdU(+) cell rate increased to 29.0% and 33.9% after 24 h of treatment with 25 μg·mL^{-1} CR and CRP, respectively. After 30 h, the cell migration rate was 28.3% in the control group and increased to 36.1% and 61.4% with 25 μg·mL^{-1} CR and CRP treatments, respectively. These results indicate that both CR and CRP promote cell proliferation and migration, with CRP showing a more pronounced effect, suggesting that sesquiterpenoids enriched in CRP are primarily responsible for the hair growth-promoting activity.

CRP was further fractionated using silica gel column chromatography to yield CRP-1 to CRP-5, effectively isolating major compounds in each fraction, as analyzed by TLC (Fig. S5). HPLC analysis revealed that cyperotundone and α-cyperone were enriched in CRP-3, while nootkatone was enriched in CRP-4 (Fig. 4B). Evaluation of IHHDPC proliferation activity by CRP-1 to CRP-5 (Fig. 5F) showed varying degrees of stimulation, with CRP-3 exhibiting the strongest activity. However, treatment with 50 μg·mL^{-1} CRP-3 increased IHHDPC viability to 143%, which was lower than that induced by 50 μg·mL^{-1} CRP (175%) under identical conditions, indicating reduced activity after fractionation. This suggests that synergistic interactions among multiple sesquiterpenoids in CRP contribute to its superior efficacy. Therefore, for subsequent animal experiments, whole CRP was selected over individual subfractions.

3.7. CR and CRP promote IHHDPC proliferation, migration and growth factor expression via Wnt/β-Catenin pathway

The specific Wnt/β-Catenin pathway inhibitor MSAB promotes β-Catenin degradation and has been reported to inhibit β-Catenin-dependent cell proliferation [51]. As shown in Figs. 6A–6D, treatment with 500 nmol·L^{-1} MSAB for 24 h did not affect IHHDPC viability but significantly downregulated intracellular β-Catenin expression. Furthermore, MSAB attenuated or abolished the pro-proliferative effects of CR and CRP on IHHDPCs. By inhibiting Wnt/β-Catenin signaling, MSAB reduced the transcription levels of *IGF1*, *KGF*, and *VEGF*, as well as IHHDPC migration capacity. Consequently, MSAB diminished or negated the stimulatory effects of CR and CRP on growth factor secretion and cell migration (Figs. 6E–6H). These findings indicate that CR and CRP promote IHHDPC proliferation, migration, and growth factor secretion

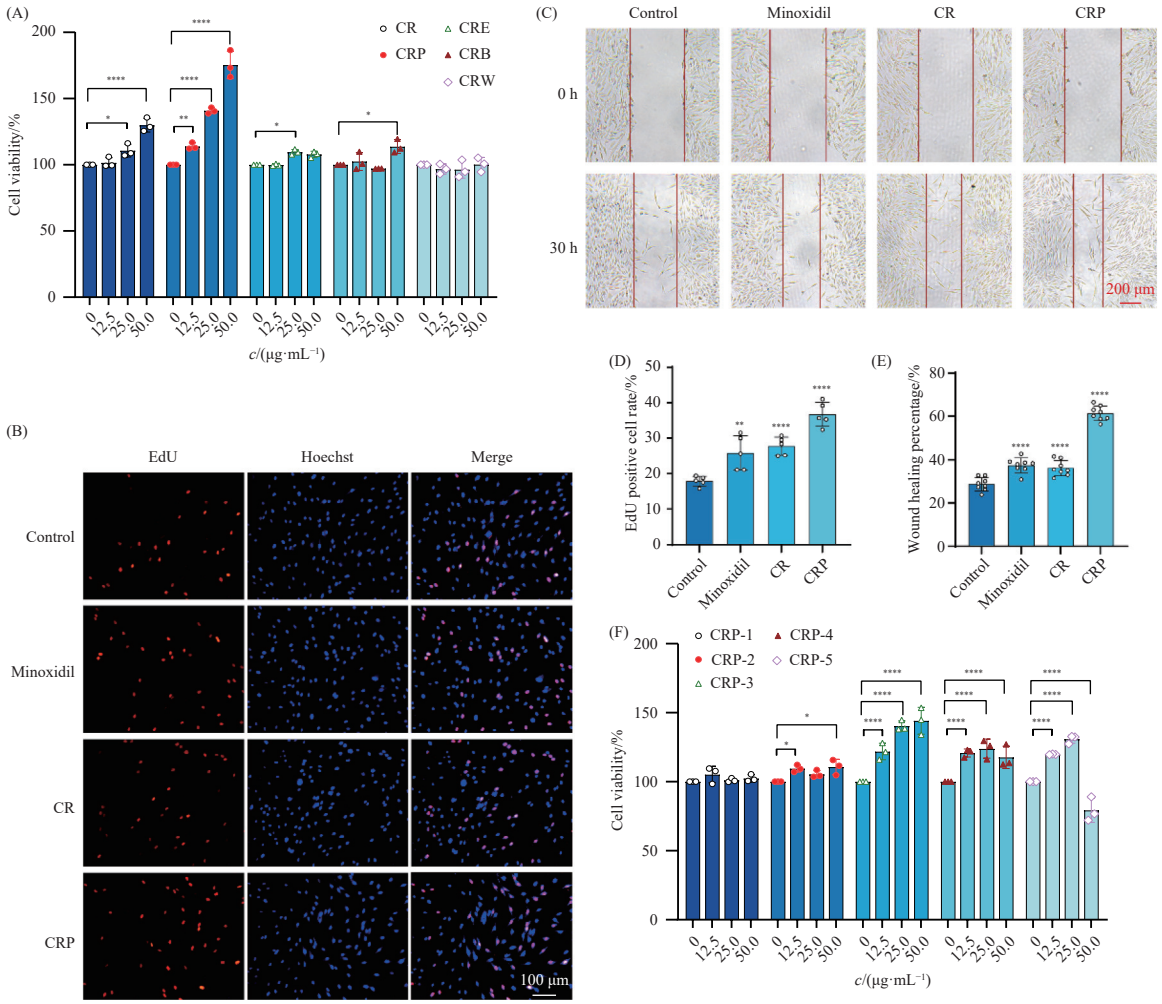

Fig. 5 Comparison of the activity of CR with its isolated extracts and fractions. (A) Effects of CR and CRP, CRE, CRB, and CRW on the viability of IHHDPCs. Effects of CR and CRP on the proliferation (B) and the migration (C) of IHHDPCs. (D and E) Quantification of the EdU(+) cell rate in (B) and cell migration rate in (C). (F) Effects of CRP-1–5 on the viability of IHHDPCs. Data are presented as mean ± SD (n = 3–5). $^{*}P < 0.05$, $^{**}P < 0.01$, $^{***}P < 0.001$, $^{****}P < 0.0001$ *vs* control by ANOVA.

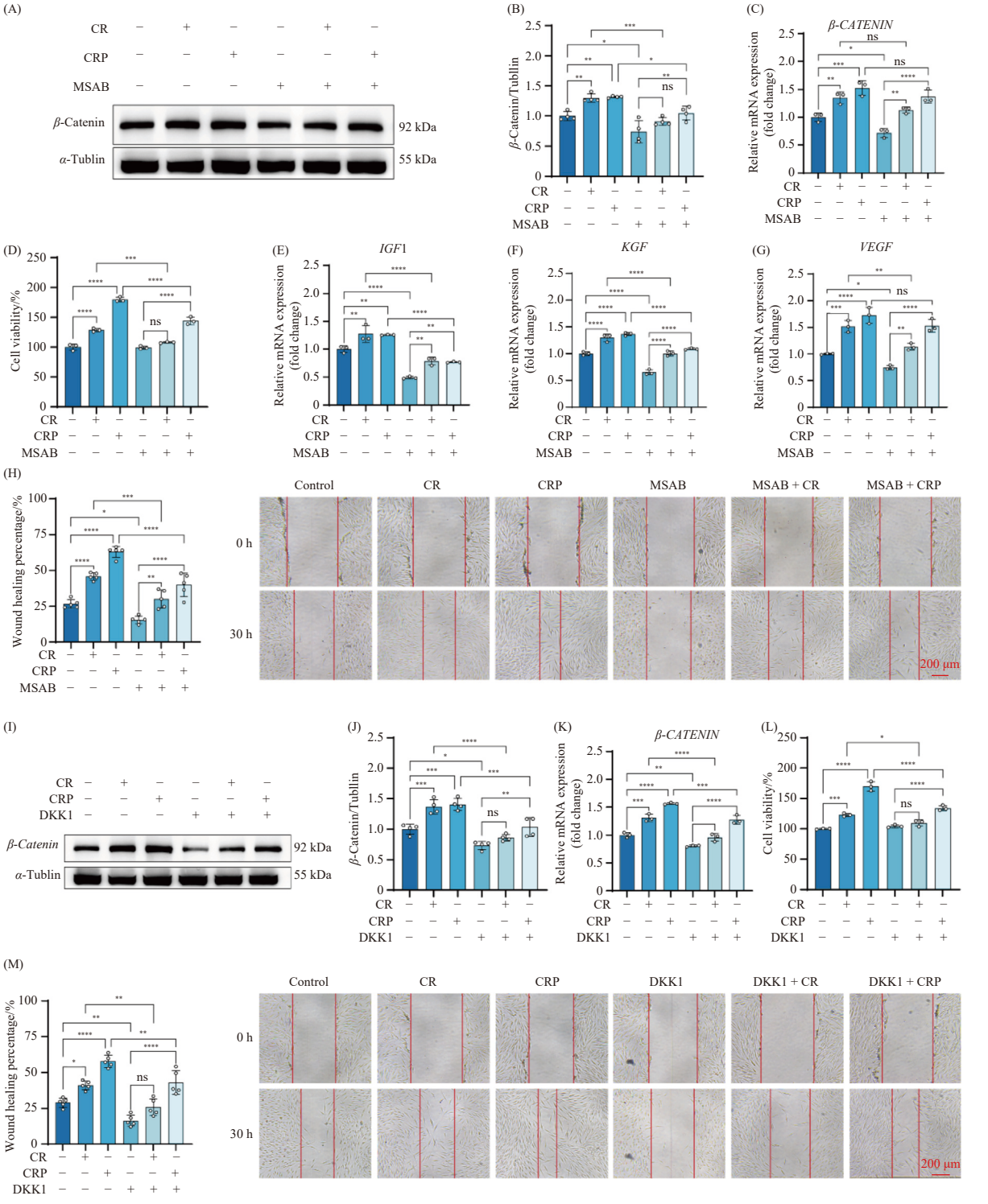

Fig. 6 Attenuated or nullified the efficacy of 50 μg·mL^{-1} CR and CRP by Wnt/β-Catenin pathway inhibition. Effects of the presence or absence of 500 nmol·L^{-1} MSAB, CR and CRP on β-Catenin protein levels (A and B), *β-CATENIN* (C), *IGF1* (E), *KGF* (F) and *VEGF* (G) mRNA level, cell viability (D), and cell migration (H) in IHHDPCs. Effects of the presence or absence of 1 μg·mL^{-1} DKK1, CR and CRP on β-Catenin protein levels (I and J), *β-CATENIN* (K) mRNA level, cell viability (L), and cell migration (M) in IHHDPCs. The data were expressed as mean ± SD (n = 3–5). $^{*}P < 0.05$, $^{**}P < 0.01$, $^{***}P < 0.001$, $^{****}P < 0.0001$ *vs* control by ANOVA.

through activation of the Wnt/β-Catenin activation.

Additionally, DKK1, an endogenous Wnt inhibitor, is upregulated during the catagen phase and induces follicle regression by suppressing Wnt/β-Catenin signaling [16]. Similar to MSAB, treatment with 1 μg·mL^{-1} DKK1 protein did not affect cell viability (Fig. 6L) but significantly reduced β-Catenin expression (Figs. 6I–6K), thereby diminishing the pro-proliferative and pro-migratory effects of CR and CRP (Figs. 6L and 6M). These findings suggest that reducing DKK1 expression facilitates Wnt/β-Catenin activation, thus sustaining the anagen phase and promoting hair growth.

3.8. CR and CRP promoted hair growth in mice

C57BL/6 mice are commonly used in hair growth research due to their synchronized HF cycles and lack of melanin production in dorsal skin. Skin color changes from pink to dark blue as melanin content increases during different hair cycle phases, al-

lowing assessment of hair growth status *via* pigmentation [52].

In this study, dorsal hair of C57BL/6 mice was removed to expose a uniform skin area (Fig. 7A). The effects of CR and CRP on hair growth were evaluated by daily topical application for 21 days, with minoxidil as a positive control. No significant differences in average body weight were observed across groups during the 21-day period (Fig. 7B). As shown in Figs. 7C and 7D, varying degrees of pigmentation appeared on mouse backs. Quantitative analysis using the mouse skin color score index on day 7 revealed that CR, CRP, and minoxidil groups exhibited more pronounced pigmentation and significantly higher scores than the control group, indicating effective induction of hair cycle reentry. Microscopic observation of subcutaneous HFs from dorsal skin collected on day 10 (Figs. 7F–7H) showed that CR, CRP, and minoxidil groups had greater HF coverage and more guard hairs in anagen phases IV–VI compared to the control. Furthermore, newly grown HFs from the depilated area on day 21 were collected and weighed. Results (Fig. 7E) demonstrated increased HS weight after treatment with CR, CRP, and minoxidil, confirming their effectiveness in promoting hair growth in mice.

3.9. Effects of CR and CRP on hair follicles and dorsal skin histology in mice

The transition from telogen to anagen is characterized by increased HF size, length, density, niche remodeling, and increased skin thickness [3,4]. To investigate the effects of CR and CRP on HF growth and development in mice, dorsal skin samples were collected on days 0, 7, 10, 14, and 21 after depilation and analyzed by H&E and Masson staining. H&E staining results (Figs. 8A–8E) showed that all mice were in the telogen phase on day 0. Transverse sections revealed that 7 days after depilation, the number of anagen HFs in dWAT layer increased, and skin thickened significantly in CR-, CRP-, and minoxidil-treated groups compared to controls. Longitudinal sections showed continuous HF elongation in all groups over 14 days. By day 14, a few HFs in the minoxidil group began to regress. By day 21, HFs in the CRPL and CRPH groups were in late catagen, while most other groups had entered telogen.

Collagen is a crucial structural component of skin and HFs, providing mechanical support essential for maintaining normal HF morphology and function, which is vital for proper hair

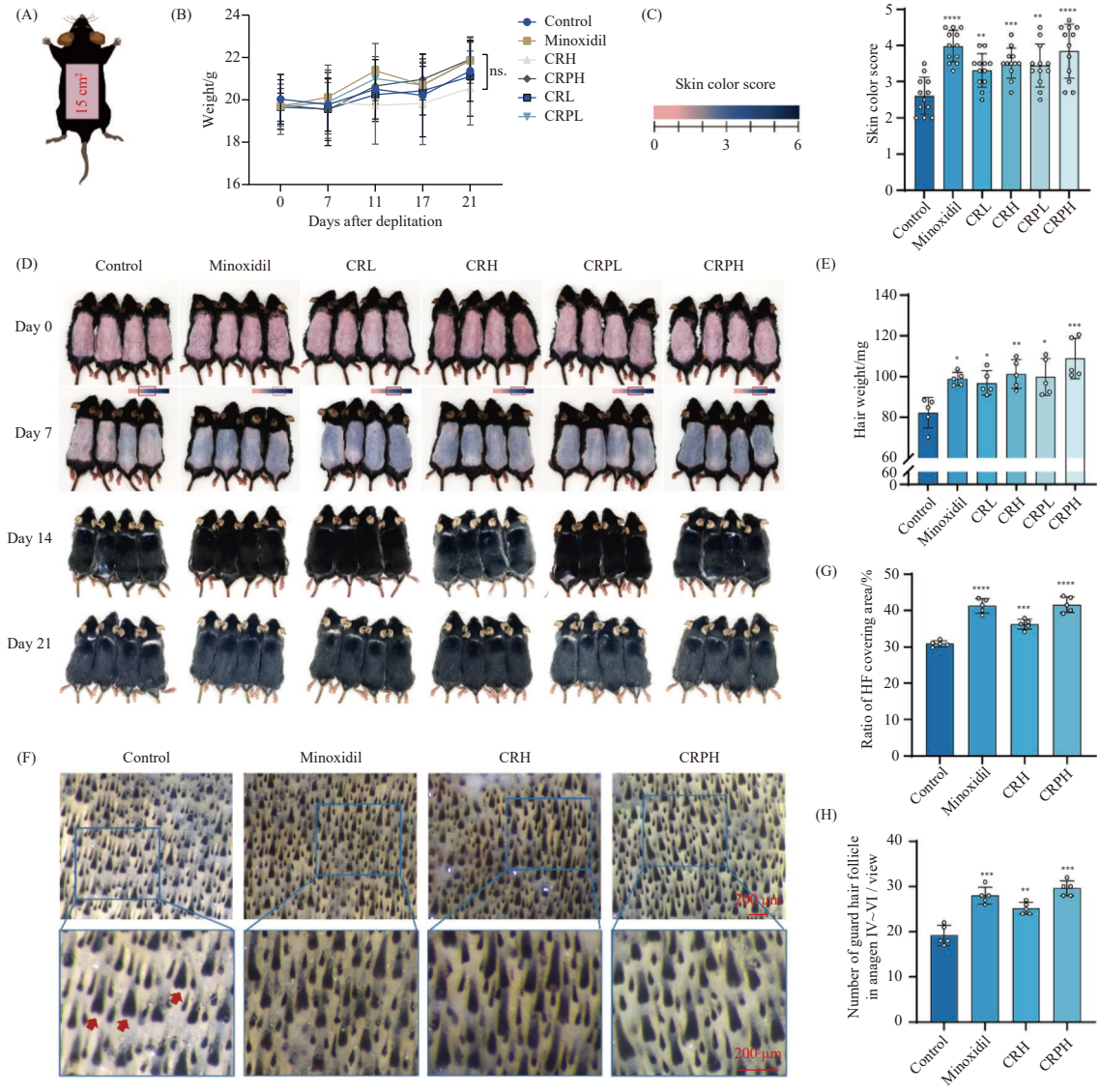

Fig. 7 Effects of CR and CRP on hair growth in C57BL/6 mice. (A) 3 cm × 5 cm wax paper was used to remove hair from the back of mice. (B) Weight change curve of mice in each group within 21 days. (C) Photos of hair growth in mice on days 0, 7, 14, and 21 after depilation. (D) Quantitative skin color score in mice on day 7 according to the mouse skin color score index (n = 12). (E) Weight of HS collected from depilated area of mice on day 21 after depilation (n = 5). (F) Microscopic observation of subcutaneous HFs of dorsal skins collected on day 10 after depilation. (G) Quantification of the ratio of HF coverage area in (F). (H) Number of guards in the anagen phase IV–VI in (F). The data were expressed as mean ± SD. $^{*}P < 0.05$, $^{**}P < 0.01$, $^{***}P < 0.001$, $^{****}P < 0.0001$ *vs* control by ANOVA.

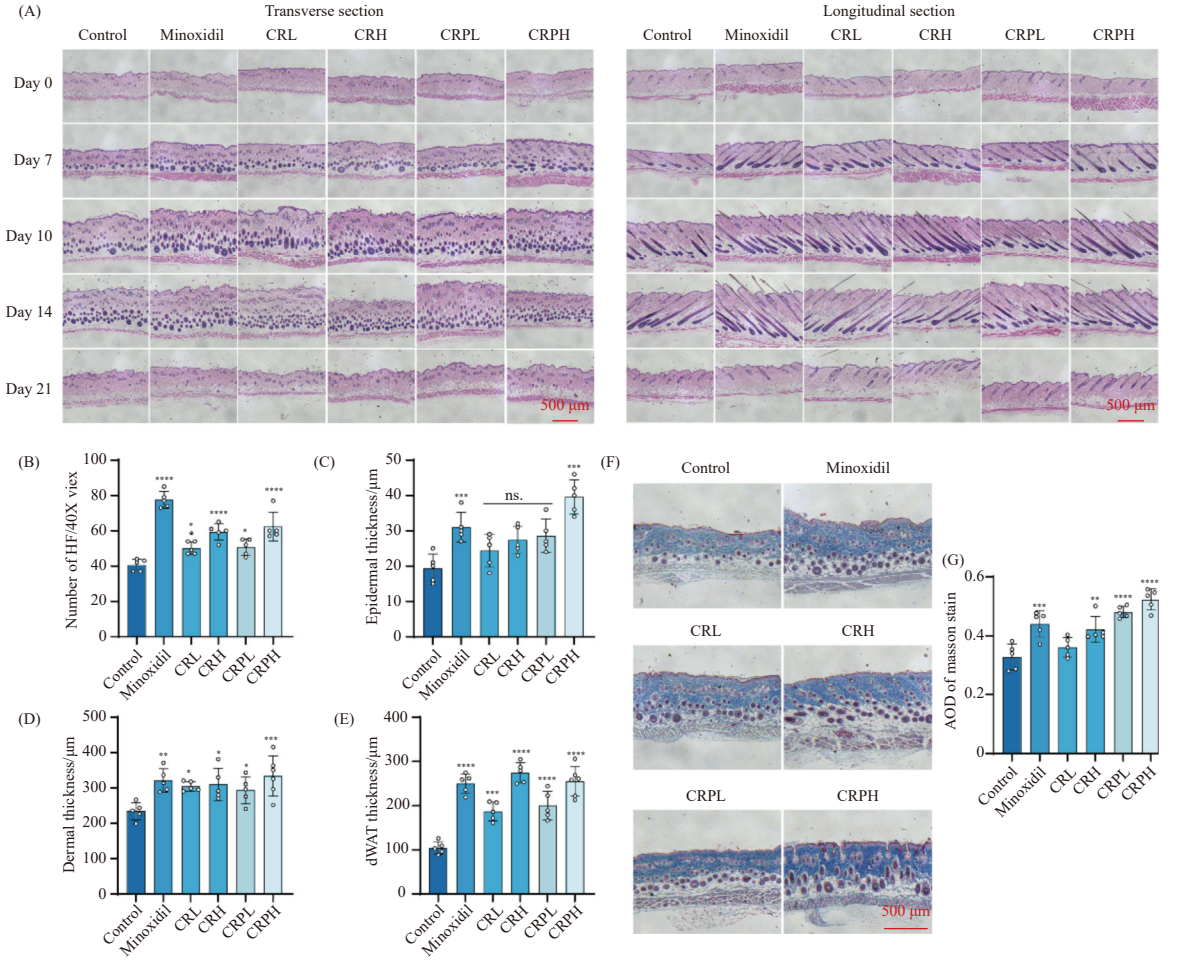

Fig. 8 Effects of CR and CRP on mouse hair follicle and skin histology. (A) H&E staining of transverse and longitudinal sections of skins. (B–E) Statistical analysis of the number of hair follicles in the dWAT layer, as well as the thickness of the epidermis, dermis, and dWAT on day 7 in (A). (F) Masson staining of transverse sections of skin on day 7, and (G) the average optical density of Masson staining. The data were expressed as mean ± SD (n = 5). $^{*}P < 0.05$, $^{**}P < 0.01$, $^{***}P < 0.001$, $^{****}P < 0.0001$ *vs* control by ANOVA.

growth and renewal [53]. To assess the effects of CR and CRP on collagen content, skin sections were subjected to Masson staining. Results (Figs. 8F and 8G) showed darker blue staining in the CR, CRP, and minoxidil groups compared to control, indicating increased collagen deposition, with the CRPH group showing the most significant enhancement.

3.10. Effects of CR and CRP on Ki67 and β-Catenin levels in HFs and dorsal skin of mice

Ki67 expression reflects cellular proliferative activity [54], and *β*-Catenin is a central mediator of the Wnt pathway, playing a critical role in maintaining hair growth [55]. Immunohistochemistry for Ki67 and *β*-Catenin was performed on skin samples collected on day 7 using specific antibodies. The results (Fig. 9) showed higher levels of Ki67 and *β*-Catenin in skin sections from the minoxidil, CRH, and CRPH groups compared to the control group.

Hair loss arises from multiple factors. In men, the most common causes include scalp androgen sensitivity and hyperandrogenemia at the vertex. In contrast, female hair loss is more complex and challenging to treat. Besides androgenic effects, factors such as postpartum changes and menopause, which lead to estrogen imbalance, can trigger telogen effluvium [56, 57]. Hair loss significantly impacts quality of life and self-esteem, posing a substantial burden for affected individuals [23]. Current FDA-approved treatments—minoxidil and finasteride—have notable side effects. Topical minoxidil may cause scalp irritation and itching, while oral minoxidil is associated with dizziness, coma, and hirsutism [24]. Finasteride has been linked to sexual dysfunction in men [24]. Hair loss primarily results from disruptions in the HF cycle and progressive HF atrophy, underscoring the importance of early intervention and consistent care. Given the limitations and adverse effects of existing therapies, they may not represent ideal long-term solutions. In contrast, natural plant extracts offer a promising alternative due to their synergistic actions, fewer side effects, and broad consumer acceptance [1, 25]. *Cyperus rotundus*, a traditional Chinese medicine with a long clinical history, has been used for gynecological and neurological disorders. Although ancient texts mention its beneficial effects on hair growth, its efficacy in treating hair loss remains unexplored [17, 29, 30]. This study confirms the efficacy of CR in promoting hair growth, providing scientific validation for its use in hair loss prevention and highlighting its potential for incorporation into anti-hair loss products and cosmetics.

HFs are complex micro-organs composed of diverse cell types. Their development and growth are regulated by interactions between DPCs and the proliferation/differentiation of other follicular cells [58]. In this study, we utilized MDPC, IHHDPC, HaCaT, and HUVEC cell models, along with *ex vivo*-cultured mouse vibrissa HFs and a C57BL/6 mouse model, to comprehensively investigate the efficacy and underlying mechanisms of CR in promoting hair growth and modulating the HF cycle at cellular, organ, and organismal levels. Following standard protocols, we first conducted LC-TOF-MS/MS to analyze the chemical composition of CR. We quantified its major constituents—cyperenone, nootkatone, and *α*-cyperone—to ensure consistent dosing. CR treatment enhanced the viability of MDPC, IHHDPC, HaCaT, and

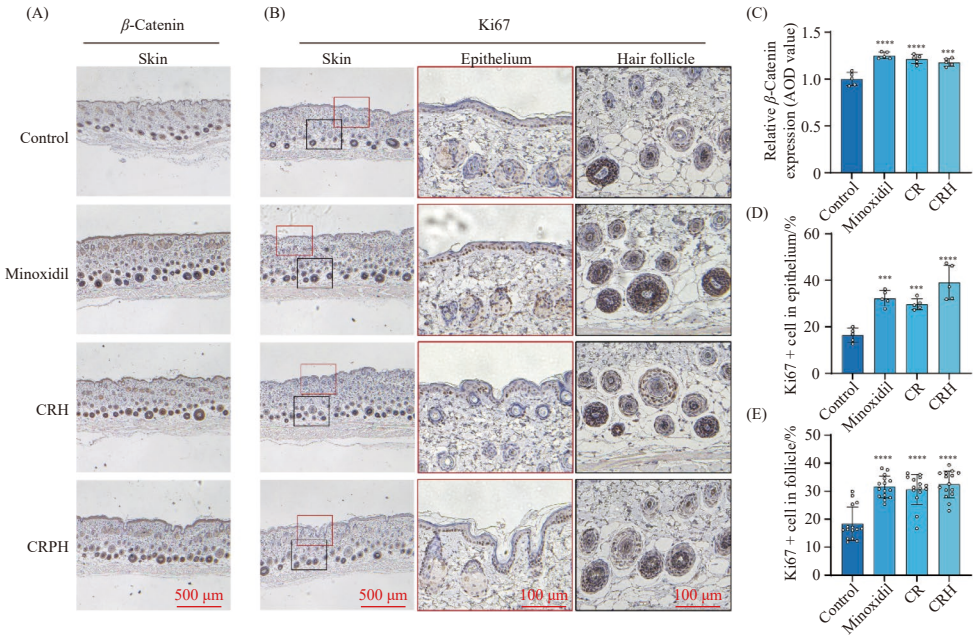

Fig. 9 Immunohistochemical analysis and quantification of *β*-Catenin (A and C) and Ki67 (B, D and E) levels in mouse dorsal skin tissue on day 7. The data were expressed as mean ± SD (n = 5). $^{***}P < 0.001$, $^{****}P < 0.0001$ *vs* control by ANOVA.

HUVEC cells and upregulated growth factor expression in MDPCs. CR maintained and prolonged the anagen phase and stimulated hair growth in both *ex vivo*-cultured mouse vibrissa HFs and *in vivo* mouse models. The underlying mechanism involves activation of the Wnt/*β*-Catenin pathway and modulation of inhibitory signals such as TGF-β1, potentially through downregulation of BMP4 signaling and reduced DKK1 expression in MDPCs. Furthermore, CRP—the sesquiterpenoid-enriched fraction of CR—demonstrated superior efficacy in IHHDPC and mouse models compared to crude CR. The effects of CR and CRP on promoting IHHDPC proliferation, migration, and growth factor secretion were mitigated or abolished by the exogenous Wnt/*β*-Catenin inhibitor MSAB and the endogenous inhibitor DKK1, underscoring the essential role of this pathway in mediating CR's effects. Reducing DKK1 expression may enhance intracellular *β*-Catenin accumulation, thereby facilitating Wnt signal transduction and promoting hair growth. To further explore active components, CRP was fractionated into five subfractions (CRP-1 to CRP-5) *via* silica gel chromatography to enrich sesquiterpenoids of varying polarities. However, component enrichment did not enhance activity; subfractions showed lower proliferative effects than CRP, and 50 μg·mL^{-1} CRP-5 even inhibited cell viability, suggesting potential synergistic interactions among multiple sesquiterpenoids in CRP. These findings highlight the need to further investigate such synergies and suggest that multi-component formulations may outperform purified fractions. Additionally, analyzing toxic constituents in CRP-5 could improve the safety profile of CRP-based preparations.

4. Conclusion

In summary, this study elucidated the role and underlying mechanisms of CR and its sesquiterpenoid-rich fraction, CRP, in promoting hair growth. A comprehensive approach was employed, encompassing chemical profiling, cell-based assays, *ex vivo* organ culture, and *in vivo* animal models. The findings demonstrate that both CR and CRP promote HF development and sustain the anagen phase by enhancing cell proliferation, regulating growth factor expression, and activating the Wnt/*β*-Catenin pathway, while simultaneously suppressing TGF-β1, BMP4, and DKK1 signaling. Notably, CRP exhibited stronger effects on cell proliferation, migration, and growth factor secretion than crude CR, indicating that sesquiterpenoids are the primary bioactive constituents. Animal experiments further confirmed that CR and CRP reactivate the hair cycle, stimulate hair growth, and improve the follicular microenvironment by increasing collagen content in mouse dorsal skin. These results provide a robust experimental foundation and theoretical framework for the application of CR and CRP in hair loss prevention and regenerative therapies.

Funding

This work was supported by the Start-up Fund of China Pharmaceutical University (No. 3150020057).

Supporting information

Supporting information of this paper, including the schematic diagram of the isolation process of primary MDPCs (Fig. S1), the identification of them (Fig. S2), the TIC of CR analysis by LC-TOF-MS/MS (Fig. S3), the primers sequences of RT-qPCR analyses in this study (Table S1), the LC-Q-TOF-MS/MS ion fragment data (Tables S2 and S3), the assay method, methodology, and result of cyperenone, *α*-cyperone, and nootkatone (Fig. S4 and Table S4), the TLC analysis of CRP-1–CRP-5 (Fig. S5), can be requested by sending E-mail to the corresponding author.

Declaration of competing interest

The authors declare no competing financial interest.

References

1 Park S, Lee J. Modulation of hair growth promoting effect by natural products. *Pharmaceutics*. 2021;13(12):2163-2187. https://doi.org/10.3390/pharmaceutics13122163.
2 Lin X, Zhu L, He J. Morphogenesis, growth cycle and molecular regulation of hair follicles. *Front Cell Dev Biol*. 2022;10:899095. https://doi.org/10.3389/fcell.2022.899095.
3 Guerrero-Juarez CF, Plikus MV. Emerging nonmetabolic functions of skin fat. *Nat Rev Endocrinol*. 2018;14(3):163-173. https://doi.org/10.1038/nrendo.2017.162.
4 Paus R, Muller-Rover S, van der Veen C, et al. A comprehensive guide for the recognition and classification of distinct stages of hair follicle morphogenesis. *J Invest Dermatol*. 1999;113(4):523-532. https://doi.org/10.1046/j.1523-1747.1999.00740.x.

5 Natarelli N, Gahoonia N, Sivamani RK. Integrative and mechanistic approach to the hair growth cycle and hair loss. *J Clin Med*. 2023;12(3):893. https://doi.org/10.3390/jcm12030893.

6 Dong TR, Li YJ, Jin SY, et al. Progress on mitochondria and hair follicle development in androgenetic alopecia: relationships and therapeutic perspectives. *Stem Cell Res Ther*. 2025;16(1):44. https://doi.org/10.1186/s13287-025-04182-z.

7 Deng Z, Chen M, Liu F, et al. Androgen receptor-mediated paracrine signaling induces regression of blood vessels in the dermal papilla in androgenetic alopecia. *J Invest Dermatol*. 2022;142(8):2088-2099. https://doi.org/10.1016/j.jid.2022.01.003.

8 Madaan A, Verma R, Singh AT, et al. Review of hair follicle dermal papilla cells as *in vitro* screening model for hair growth. *Int J Cosmetic Sci*. 2018;40(5):429-450. https://doi.org/10.1111/ics.12489.

9 Gentile P, Garcovich S. Advances in regenerative stem cell therapy in androgenic alopecia and hair loss: Wnt pathway, growth-factor, and mesenchymal stem cell signaling impact analysis on cell growth and hair follicle development. *Cells-Basel*. 2019;8(5):466-487. https://doi.org/10.3390/cells8050466.

10 Huang P, Yan R, Zhang X, et al. Activating Wnt/*β*-Catenin signaling pathway for disease therapy: challenges and opportunities. *Pharmacol Therapeut*. 2019;196:79-90. https://doi.org/10.1016/j.pharmthera.2018.11.008.

11 Lim X, Nusse R. Wnt signaling in skin development, homeostasis, and disease. *Csh Perspect Biol*. 2013;5(2):a8029. https://doi.org/10.1101/cshperspect.a008029.

12 Liu J, Mu Q, Liu Z, et al. Melatonin regulates the periodic growth of cashmere by upregulating the expression of Wnt10b and *β*-Catenin in inner mongolia cashmere goats. *Front Genet*. 2021;12:665834. https://doi.org/10.3389/fgene.2021.665834.

13 Lei M, Lai X, Bai X, et al. Prolonged overexpression of Wnt10b induces epidermal keratinocyte transformation through activating EGF pathway. *Histochem Cell Biol*. 2015;144(3):209-221. https://doi.org/10.1007/s00418-015-1330-6.

14 Zhao B, Li J, Zhang X, et al. Exosomal miRNA-181a-5p from the cells of the hair follicle dermal papilla promotes the hair follicle growth and development *via* the Wnt/*β*-Catenin signaling pathway. *Int J Biol Macromol*. 2022;207:110-120. https://doi.org/10.1016/j.ijbiomac.2022.02.177.

15 Enshell-Seijffers D, Lindon C, Kashiwagi M, et al. *β*-Catenin activity in the dermal papilla regulates morphogenesis and regeneration of hair. *Dev Cell*. 2010;18(4):633-642. https://doi.org/10.1016/j.devcel.2010.01.016.

16 Rishikaysh P, Dev K, Diaz D, et al. Signaling involved in hair follicle morphogenesis and development. *Int J Mol Sci*. 2014;15(1):1647-1670. https://doi.org/10.3390/ijms15011647.

17 Dou J, Zhang Z, Xu X, et al. Exploring the effects of Chinese herbal ingredients on the signaling pathway of alopecia and the screening of effective Chinese herbal compounds. *J Ethnopharmacol*. 2022;294(10):115320. https://doi.org/10.1016/j.jep.2022.115320.

18 Plikus MV, Mayer JA, de la CD, et al. Cyclic dermal BMP signalling regulates stem cell activation during hair regeneration. *Nature*. 2008;451(7176):340-344. https://doi.org/10.1038/nature06457.

19 Greco V, Chen T, Rendl M, et al. A two-step mechanism for stem cell activation during hair regeneration. *Cell Stem Cell*. 2009;4(2):155-169. https://doi.org/10.1016/j.stem.2008.12.009.

20 Vasserot AP, Geyfman M, Poloso NJ. Androgenetic alopecia: combing the hair follicle signaling pathways for new therapeutic targets and more effective treatment options. *Expert Opin Ther Tar*. 2019;23(9):755-771. https://doi.org/10.1080/14728222.2019.1659779.

21 Bayati P, Taherian M, Soleimani M, et al. Induced pluripotent stem cells modulate the Wnt pathway in the bleomycin-induced model of idiopathic pulmonary fibrosis. *Stem Cell Res Ther*. 2023;14(1):343. https://doi.org/10.1186/s13287-023-03581-4.

22 Kamiya N. The role of BMPs in bone anabolism and their potential targets sost and DKK1. *Curr Mol Pharmacol*. 2012;5(2):153-163. https://doi.org/10.2174/1874467211205020153.

23 Alessandrini A, Bruni F, Piraccini BM, et al. Common causes of hair loss-clinical manifestations, trichoscopy and therapy. *J Eur Acad Dermatol*. 2021;35(3):629-640. https://doi.org/10.1111/jdv.17079.

24 Devjani S, Ezemma O, Kelley KJ, et al. Androgenetic alopecia: therapy update. *Drugs*. 2023;83(8):701-715. https://doi.org/10.1007/s40265-023-01880-x.

25 Choi JY, Boo MY, Boo YC. Can plant extracts help prevent hair loss or promote hair growth? A review comparing their therapeutic efficacies, phytochemical components, and modulatory targets. *Molecules*. 2024;29(10):2288. https://doi.org/10.3390/molecules29102288.

26 Hwang SB, Park HJ, Lee BH. Hair-growth-promoting effects of the fish collagen peptide in human dermal papilla cells and C57BL/6 mice modulating Wnt/*β*-Catenin and BMP signaling pathways. *Int J Mol Sci*. 2022;23(19):11904. https://doi.org/10.3390/ijms231911904.

27 Datta K, Singh AT, Mukherjee A, et al. *Eclipta Alba* extract with potential for hair growth promoting activity. *J Ethnopharmacol*. 2009;124(3):450-456. https://doi.org/10.1016/j.jep.2009.05.023.

28 Iwabuchi T, Ogura K, Hagiwara K, et al. Ginsenosides in *Panax Ginseng* extract promote anagen transition by suppressing BMP4 expression and promote human hair growth by stimulating follicle-cell proliferation. *Biol Pharm Bull*. 2024;47(1):240-244. https://doi.org/10.1248/bpb.b23-00276.

29 Peerzada AM, Ali HH, Naeem M, et al. *Cyperus Rotundus* L.: traditional uses, phytochemistry, and pharmacological activities. *J Ethnopharmacol*. 2015;174(4):540-560. https://doi.org/10.1016/j.jep.2015.08.012.

30 Xue BX, He RS, Lai JX, et al. Phytochemistry, data mining, pharmacology, toxicology and the analytical methods of *Cyperus Rotundus* L. (Cyperaceae): a comprehensive review. *Phytochem Rev*. 2023;2023:1-46. https://doi.org/10.1007/s11101-023-09870-3.

31 Zhang H, Shi Q, Nan W, et al. Ginkgolide B and bilobalide promote the growth and increase *β*-Catenin expression in hair follicle dermal papilla cells of American minks. *Biofactors*. 2019;45(6):950-958. https://doi.org/10.1002/biof.1562.

32 Topouzi H, Logan NJ, Williams G, et al. Methods for the isolation and 3D culture of dermal papilla cells from human hair follicles. *Exp Dermatol*. 2017;26(6):491-496. https://doi.org/10.1111/exd.13368.

33 Gan Y, Wang H, Du L, et al. Ficoll density gradient sedimentation isolation of pelage hair follicle mesenchymal stem cells from adult mouse back skin: a novel method for hair follicle mesenchymal stem cells isolation. *Stem Cell Res Ther*. 2022;13(1):372-385. https://doi.org/10.1186/s13287-022-03051-3.

34 Limbu S, Higgins CA. Isolating dermal papilla cells from human hair follicles using microdissection and enzyme digestion. *Methods Mol Biol*. 2020;2154:91-103. https://doi.org/10.1007/978-1-0716-0648-3_8.

35 Yang CC, Cotsarelis G. Review of hair follicle dermal cells. *J Dermatol Sci*. 2010;57(1):2-11. https://doi.org/10.1016/j.jdermsci.2009.11.005.

36 Ha EJ, Yun JH, Si C, et al. Application of ethanol extracts from *Alnus Sibirica* Fisch. Ex Turcz in hair growth promotion. *Front Bioeng Biotech*. 2021;9:673314. https://doi.org/10.3389/fbioe.2021.673314.

37 Fu D, Huang J, Li K, et al. Dihydrotestosterone-induced hair regrowth inhibition by activating androgen receptor in C57BL/6 mice simulates androgenetic alopecia. *Biomed Pharmacother*. 2021;137:111247. https://doi.org/10.1016/j.biopha.2021.111247.

38 Fu H, Li W, Weng Z, et al. Water extract of *Cacumen platycladi* promotes hair growth through the Akt/Gsk3β/*β*-Catenin signaling pathway. *Front Pharmacol*. 2023;14:1038039. https://doi.org/10.3389/fphar.2023.1038039.

39 Morgan BA. The dermal papilla: an instructive niche for epithelial stem and progenitor cells in development and regeneration of the hair follicle. *Csh Perspect Med*. 2014;4(7):a15180. https://doi.org/10.1101/cshperspect.a015180.

40 Junlatat J, Sripanidkulchai B. Hair growth-promoting effect of *Carthamus tinctorius* floret extract. *Phytother Res*. 2014;28(7):1030-1036. https://doi.org/10.1002/ptr.5100.

41 Li Y, Sheng Y, Liu J, et al. Hair-growth promoting effect and anti-inflammatory mechanism of *Ginkgo biloba* polysaccharides. *Carbohyd Polym*. 2022;278(15):118811. https://doi.org/10.1016/j.carbpol.2021.118811.

42 Hyun J, Im J, Kim S, et al. *Morus alba* root extract induces the anagen phase in the human hair follicle dermal papilla cells. *Pharmaceutics*. 2021;13(8):1155. https://doi.org/10.3390/pharmaceutics13081155.

43 Lee E, Seo HD, Kim D, et al. Millet seed oil activates *β*-Catenin signaling and promotes hair growth. *Front Pharmacol*. 2023;14:1172084. https://doi.org/10.3389/fphar.2023.1172084.

44 Ryu YC, Lee DH, Shim J, et al. KY19382, a novel activator of Wnt/*β*-Catenin signaling, promotes hair regrowth and hair follicle neogenesis. *Brit J Pharmacol*. 2021;178(12):2533-2546. https://doi.org/10.1111/bph.15438.

45 Choi BY. Targeting Wnt/*β*-catenin pathway for developing therapies for hair loss. *Int J Mol Sci*. 2020;21(14):4915-4931. https://doi.org/10.3390/ijms21144915.

46 Papukashvili D, Rcheulishvili N, Liu C, et al. Perspectives on miRNAs targeting DKK1 for developing hair regeneration therapy. *Cells-Basel*. 2021;10(11):2957-2993. https://doi.org/10.3390/cells10112957.

47 Robinson M, Reynolds AJ, Jahoda CA. Hair cycle stage of the mouse vibrissa follicle determines subsequent fiber growth and follicle behavior *in vitro*. *J Invest Dermatol*. 1997;108(4):495-500. https://doi.org/10.1111/1523-1747.ep12289730.

48 Muller-Rover S, Handjiski B, van der Veen C, et al. A comprehensive guide for the accurate classification of murine hair follicles in distinct hair cycle stages. *J Invest Dermatol*. 2001;117(1):3-15. https://doi.org/10.1046/j.0022-202x.2001.01377.x.

49 Kim J, Kim SR, Choi YH, et al. Quercitrin stimulates hair growth with enhanced expression of growth factors *via* activation of MAPK/CREB signaling pathway. *Molecules*. 2020;25(17):4004-4018. https://doi.org/10.3390/molecules25174004.

50 Shin K, Choi H, Song SK, et al. Nanoemulsion vehicles as carriers for follicular delivery of luteolin. *Acs Biomater Sci Eng*. 2018;4(5):1723-1729. https://doi.org/10.1021/acsbiomaterials.8b00220.

51 Hwang SY, Deng X, Byun S, et al. Direct targeting of *β*-Catenin by a small molecule stimulates proteasomal degradation and suppresses oncogenic Wnt/*β*-Catenin signaling. *Cell Rep*. 2016;16(1):28-36. https://doi.org/10.1016/j.celrep.2016.05.071.

52 Ohn J, Kim KH, Kwon O. Evaluating hair growth promoting effects of candidate substance: a review of research methods. *J Dermatol Sci*. 2019;93(3):144-149. https://doi.org/10.1016/j.jdermsci.2019.02.004.

53 Williams R, Pawlus AD, Thornton MJ. Getting under the skin of hair aging: the impact of the hair follicle environment. *Exp Dermatol*. 2020;29(7):588-597. https://doi.org/10.1111/exd.14109.

54 Han M, Li C, Zhang C, et al. Single-cell transcriptomics reveals the natural product Shi-Bi-Man promotes hair regeneration by activating the FGF pathway in dermal papilla cells. *Phytomedicine*. 2022;104:154260. https://doi.org/10.1016/j.phymed.2022.154260.

55 Tang X, Zhang T, Wang B, et al. Biotransformation of *Cacumen platycladi* extract by *Lactiplantibacillus plantarum* CCFM1348 promotes hair growth in mice. *J Agr Food Chem*. 2024;72(20):11493. https://doi.org/10.1021/acs.jafc.4c00807.

56 Bertoli MJ, Sadoughifar R, Schwartz RA, et al. Female pattern hair loss: a comprehensive review. *Dermatol Ther*. 2020;33(6):e14055. https://doi.org/10.1111/dth.14055.

57 Shapiro J. Clinical practice. Hair loss in women. *New Engl J Med*. 2007;357(16):1620-1630. https://doi.org/10.1056/NEJMcp072110.

58 Cuevas-Diaz DR, Martinez-Ledesma E, Garcia-Garcia M, et al. The biology and genomics of human hair follicles: a focus on androgenetic alopecia. *Int J Mol Sci*. 2024;25(5):2542. https://doi.org/10.3390/ijms25052542.